

Dihydropyridine-insensitive calcium currents contribute to function of small cerebral arteries

Ivana Y Kuo¹, Anthie Ellis^{1,3}, Victoria AL Seymour^{1,3}, Shaun L Sandow² and Caryl E Hill¹

¹Neuroscience Program, John Curtin School of Medical Research, ANU College of Medicine, Biology and Environment, The Australian National University, Canberra, Australian Capital Territory, Australia; ²Department of Pharmacology, School of Medical Sciences, University of New South Wales, Kensington, New South Wales, Australia

Although dihydropyridines are widely used for the treatment of vasospasm, their effectiveness is questionable, suggesting that other voltage-dependent calcium channels (VDCCs) contribute to control of cerebrovascular tone. This study therefore investigated the role of dihydropyridine-insensitive VDCCs in cerebrovascular function. Using quantitative PCR and immunohistochemistry, we found mRNA and protein for L-type ($Ca_v1.2$) and T-type ($Ca_v3.1$ and $Ca_v3.2$) channels in adult rat basilar and middle cerebral arteries and their branches. Immunoelectron microscopy revealed both L- and T-type channels in smooth muscle cell (SMC) membranes. Using patch clamp electrophysiology, we found that a high-voltage-activated calcium current, showing T-type channel kinetics and insensitivity to nifedipine and nimodipine, comprised ~20% of current in SMCs of the main arteries and ~45% of current in SMCs from branches. Both components were abolished by the T-type antagonists mibefradil, NNC 55-0396, and efonidipine. Although nifedipine completely blocked vasoconstriction in pressurized basilar arteries, a nifedipine-insensitive constriction was found in branches and this increased in magnitude as vessel size decreased. We conclude that a heterogeneous population of VDCCs contributes to cerebrovascular function, with dihydropyridine-insensitive channels having a larger role in smaller vessels. Sensitivity of these currents to nonselective T-type channel antagonists suggests that these drugs may provide a more effective treatment for therapy-refractory cerebrovascular constriction.

Journal of Cerebral Blood Flow & Metabolism (2010) 30, 1226–1239; doi:10.1038/jcbfm.2010.11; published online 3 February 2010

Keywords: arterial size; calcium channels; cerebral vasoconstriction; dihydropyridines; T-type channels

Introduction

Although subarachnoid haemorrhage accounts for only 5% to 10% of all strokes, the prognosis is poor due to the high incidence of subsequent cerebral ischaemia resulting from arterial vasospasm. While antagonism of L-type voltage-dependent calcium channels (VDCCs) forms the mainline treatment for vasospasm, the effectiveness of these drugs in improving patient outcome in terms of morbidity and mortality is questionable. In a recent assessment of the results from clinical trials of calcium channel

antagonists, only oral administration of the highly lipophilic blocker, nimodipine, had a significant effect in improving patient outcome, although this effect was not seen when data from one large study were excluded (Dorhout Mees *et al*, 2007). Interestingly, the improvement in neurological outcome was not accompanied by angiographic evidence of the prevention or reversal of arterial spasm (Tomassoni *et al*, 2008). Although the lack of effect of nimodipine and other L-type VDCC antagonists on vasospasm could be attributable to inadequate dose due to the associated risk of harmful blood pressure lowering or other side effects, it is also possible that additional subtypes of VDCCs contribute to cerebral vasoconstriction.

Recent studies have provided evidence that T-type channels are expressed in basilar, mesenteric, renal, cremaster, and subcutaneous resistance arteries, and nifedipine-insensitive currents have been reported to contribute to vascular responses (Ball *et al*, 2009; Braunstein *et al*, 2008; Jensen *et al*, 2004; Morita *et al*, 2002; Navarro-Gonzalez *et al*, 2009; Nikitina *et al*, 2007; VanBavel *et al*, 2002). However, a role

Correspondence: Professor CE Hill, Neuroscience Program, John Curtin School of Medical Research, ANU College of Medicine, Biology and Environment, The Australian National University, GPO Box 334, Canberra, ACT 0200, Australia.
E-mail: caryl.hill@anu.edu.au

³These authors contributed equally to this work.

This work was supported by National Health and Medical Research Council of Australia (471420 and 401112) and by Australian Research Council (DP0663818).

Received 21 November 2009; revised 7 January 2010; accepted 10 January 2010; published online 3 February 2010

for the traditionally low-voltage-activated T-type channels seems unlikely, because the window current of T-type calcium channels lies between -70 and -65 mV (Perez-Reyes, 2003), outside the range of potentials experienced by smooth muscle cells (SMCs) of arteries at physiological pressures (-60 to -40 mV, Knot and Nelson, 1998).

Nevertheless, T-type channels have been implicated in blood pressure regulation because mibefradil, which was described as a selective inhibitor of T-type channels (Clozel *et al*, 1997) and marketed for treatment of essential hypertension and stable angina pectoris, was found to be highly effective in short-term clinical trials and animal studies (Baylis *et al*, 2001; Beltrame *et al*, 2004; Ertel *et al*, 1997; Vacher *et al*, 1996; Van der Vring *et al*, 1999). Although mibefradil was withdrawn due to adverse interactions with other drugs in a small group of patients, subsequent studies of mibefradil and other putative T-type VDCC blockers have shown nonspecific effects on L-type VDCCs and other channels, particularly at higher concentrations (Heady *et al*, 2001). Indeed, recent murine studies of conditional deletion of the L-type channel, $Ca_v1.2$, in SMCs suggest that the effects of mibefradil are entirely mediated by L-type channels (Moosmang *et al*, 2006). Mibefradil significantly reduced mean arterial pressure and increased flow in a perfused hindlimb preparation of wild-type mice, but failed to affect flow or pressure in SMC $Ca_v1.2$ knockout mice (Moosmang *et al*, 2006). However, the authors of this study also reported paradoxical increases in heart rate by mibefradil in both control mice and those lacking SMC $Ca_v1.2$. Although this reflex tachycardia, presumably associated with reduced peripheral resistance, would be expected in L-type channel expressing wild-type mice, parallel effects in the SMC $Ca_v1.2$ knockouts cannot be ascribed to a vasodilatory action on $Ca_v1.2$ channel, suggesting therefore an action on another calcium channel. This accords with previous studies of mesenteric vessels in which nifedipine-insensitive currents were reported to be more prominent in terminal mesenteric arterioles (Morita *et al*, 1999; Morita *et al*, 2002), as was expression of T-type VDCCs (Gustafsson *et al*, 2001; Jensen *et al*, 2004). T-type VDCCs were also increased in expression relative to L-type channels in mesenteric arteries, compared with the aorta, and a non-L-type component of endothelin constriction described (Ball *et al*, 2009).

The role of a non-L-type VDCC in the cerebral circulation, however, is controversial. The majority of studies reporting calcium currents recorded from isolated cerebral SMCs have failed to identify a low-voltage-activated component (McHugh and Beech, 1996; Worley *et al*, 1991), and the myogenic response of posterior cerebral arteries is abolished by dihydropyridine antagonists of L-type channels (Knot and Nelson, 1998). However, a low-voltage-activated current has been reported in SMCs from the adult dog basilar artery, in which the T-type VDCCs, $Ca_v3.1$

and 3.3 , were expressed (Nikitina *et al*, 2007), whereas a nifedipine-insensitive VDCC has been shown to control vascular tone of juvenile rat basilar arteries (Navarro-Gonzalez *et al*, 2009), in which $Ca_v3.1$ and 3.2 were expressed. Given these data, we reinvestigated in this study a role for dihydropyridine-insensitive VDCCs in cerebrovascular function, paying particular attention to vessels of different calibre. Thus, we examined the distribution of VDCC subtypes in the adult rat basilar and middle cerebral arterial circulations. In addition, the effects of L-type antagonists and the putative T-type blockers (mibefradil, NNC 55-0396, and efonidipine) (Braunstein *et al*, 2008; Furukawa *et al*, 2004; Huang *et al*, 2004) on VDCC currents of isolated cerebrovascular SMCs were correlated with effects on myogenic constriction of pressurized cerebral arteries of different size.

Materials and methods

Animals

Male Wistar rats (240 to 280 g) were anaesthetized with isoflurane and decapitated (mRNA, electrophysiology, pressure myography), or injected intraperitoneally with ketamine and xylazine (44 and 8 mg/kg; immunohistochemistry, immunoelectron microscopy). All protocols were approved by the Animal Experimentation Ethics Committee of the Australian National University.

RNA Extraction and RT-PCR

Basilar arteries or middle cerebral arteries (MCAs) and their branches were removed from the surface of the brain, isolated from all adherent meninges, cleared of blood and pooled separately from 8 to 12 rats. mRNA was extracted using RNeasy mini column extraction kit with on-column DNase treatment (Qiagen, Valencia, CA, USA) and reverse transcribed into cDNA, as described previously (Navarro-Gonzalez *et al*, 2009). Reverse transcriptase was omitted from parallel samples.

Semi-quantitative PCR, with subtype-specific primers (Navarro-Gonzalez *et al*, 2009), was used to screen for expression of all 10 Ca_v subtypes in arterial samples of basilar arteries, MCAs, and their branches ($n=4$ preparations for each sample). Subsequently, for those subtypes that were commonly detected, expression levels were quantified using real-time PCR and SYBR Green core reagents. Melt curves were run to ensure sample purity. To normalize data for comparisons of expression among different Ca_v subtypes, we expressed copy numbers in each preparation relative to the content of 18S ribosomal RNA.

Immunohistochemistry

Rats were perfused transcardially with saline containing 0.1% $NaNO_2$, 0.1% bovine serum albumin (Sigma, Castle Hill, Australia), and heparin (Sigma), and decapitated.

Basilar arteries, MCAs, and their branches were removed, immersed in 30% sucrose (10 min), and incubated in rabbit anti-Ca_v1.2 (1:300), anti-Ca_v1.3 (1:200), anti-Ca_v2.1 (1:400), anti-Ca_v2.3 (1:500; Alomone, Jerusalem, Israel), anti-Ca_v3.1 (1:500) or anti Ca_v3.2 (1:300; kindly provided by Dr Leanne Cribbs, Loyola University, Chicago, IL, USA) in 2% bovine serum albumin, 0.2% Triton X in PBS (24 to 48 h, 4°C) and visualized using donkey anti-rabbit Alexa Fluor 488 (1:200; Molecular Probes, Invitrogen, Eugene, OR, USA). Cell nuclei were stained with propidium iodide (0.001% w/v H₂O). Antibodies against Ca_v3.1 and 3.2 have been previously tested for specificity using transfected HEK cells (Rodman *et al*, 2005), whereas the specificities of Ca_v1.2 and 2.3 antibodies have been previously shown by western blot (Nikitina *et al*, 2007). Isolated SMCs were fixed in 2% paraformaldehyde (10 min) and processed similarly.

To ensure primary antibody specificity, we exposed vessel segments to primary antibodies previously incubated with an excess of the immunizing peptide (1 h, RT).

Preparations were viewed with a confocal microscope (Axioskop II; Zeiss Instruments, Heidelberg, Germany). Optical z-axis sections were collected at 0.3 or 1 μm intervals. Control slides were scanned using the same settings as corresponding experimental samples.

Immunoelectron Microscopy

Segments of basilar artery side branches (1 to 2 mm long) were rapidly dissected from heavily anaesthetized rats and transferred to 1-mm-deep planchets in Krebs solution (mmol/L): 120 NaCl, 5 KCl, 25 NaHCO₃, 1 NaH₂PO₄, 2.5 CaCl₂, 2 MgCl₂, 11 glucose, gassed with 95% O₂ and 5% CO₂ for high-pressure freezing (Balzers HPM010, Liechtenstein) at ~2100 bar, as previously described (Haddock *et al*, 2006). Tissue was then freeze substituted (Leica AFS, Vienna, Austria) over 4 days to -90°C in 0.1% uranyl acetate in acetone and embedded in LR Gold, polymerized under UV light at -25°C. Serial transverse sections (~100 nm thick) were cut and processed for immunohistochemistry as above, using secondary antibodies conjugated to colloidal gold (5, 10 nm; ProSciTech, Thuringowa, QLD, Australia). Sections were imaged at ×10,000 to ×40,000 on a Phillips 7100 transmission electron microscope using a 16 megapixel resolution camera (Scientific Instruments and Applications, Duluth, MN, USA).

Patch Clamp Electrophysiology

Basilar arteries, MCAs, or their side branches were stripped of meninges and incubated sequentially at 37°C in 0.8 mg/mL papain (Worthington, Lakewood, NJ, USA), 1.6 mg/mL dithiothreitol (Sigma), and 10 U/mL DNase in physiological salt solution containing 140 mmol/L NaCl, 5 mmol/L KCl, 1 mmol/L MgCl₂, 10 mmol/L glucose, 10 mmol/L 4-(2-hydroxyethyl)-1-piperazineethanesulfonic acid (HEPES), 0.01 mmol/L sodium nitroprusside, 0.01 mmol/L CaCl₂, 1% bovine serum albumin, followed by 1.5 mg/mL collagenase and 10 U/mL DNase (15 min each). Vessel segments were washed, triturated to individual SMCs, plated on coverslips, and used within 5 h.

Whole-cell currents were recorded at RT using borosilicate pipettes (resistance 5 to 7 MΩ, P-87 Flaming Brown; Sutter Instruments, Novato, CA, USA; Axopatch 200 A amplifier, Axon Instruments, Sunnyvale, CA, USA). Series resistance was <20 MΩ and cell capacitance 8 to 15 pF. As whole-cell currents recorded in these experiments were small <200 pA, the voltage drop across the electrode series resistance was minimal (<3 mV), hence series resistance compensation was not applied. Activation protocols from holding potentials of -50, -70, and -100 mV comprised 100 ms depolarizing steps from -50 to +50 mV (Axograph X; Axograph Scientific, Sydney, Australia). Inactivation protocols used a conditioning step to potentials from -60 to +10 mV, returning to holding potential (10 ms), followed by step to +10 mV (100 ms). For channel deactivation, tail currents were evoked by a step to +10 mV (20 ms) and hyperpolarization to -100 mV. Current records were low-pass filtered at 2 or 10 kHz and digitized at 4 or 50 kHz (Digidata 1322A; Axon Instruments). Leak currents were subtracted online from all measurements by scaling a 10-mV hyperpolarizing prepulse, repeated four times, to the size of the test pulse.

Initial bath solution comprised 145 mmol/L NaCl, 10 mmol/L BaCl₂, 10 mmol/L HEPES, 10 mmol/L glucose, and 5 mmol/L CsCl. After seal formation, the 145 mmol/L NaCl was replaced with 135 mmol/L NaCl and 10 mmol/L tetraethylammonium-Cl. In some experiments, 10 mmol/L BaCl₂ was replaced with 2 mmol/L CaCl₂ and 5 mmol/L 4-aminopyridine to block voltage-dependent potassium channels. Pipette solution contained 110 mmol/L CsCl, 20 mmol/L Na₂-phosphocreatine, 10 mmol/L EGTA, 5 mmol/L Na₂ATP, 5 mmol/L MgCl₂, 0.2 mmol/L NaGTP, and 10 mmol/L HEPES. The pH (7.2) of pipette solutions was adjusted using CsOH. Osmolarity was 310 to 325 mOsm.

Effects of drugs were determined in the same cell by comparing currents before, during, and after drug application.

Pressure Myography

Segments of the main basilar artery (319 ± 8 μm; n = 4) and its larger (172 ± 4 μm; n = 17) and smaller branches (103 ± 4 μm, n = 6) were equilibrated for 1 h at 70 mm Hg (Living Systems Instruments, Burlington, VT, USA) to develop myogenic tone while superfused with physiological solution: 118 mmol/L NaCl, 4.7 mmol/L KCl, 25 mmol/L NaHCO₃, 1.0 mmol/L KH₂PO₄, 2.5 mmol/L CaCl₂, 0.45 mmol/L MgSO₄, 11.1 mmol/L glucose, bubbled with 5% CO₂/95% air at 36°C. Pressure-response curves were determined from 20 to 120 mm Hg (branches) or 20 to 160 mm Hg (main arteries) and repeated in drugs. Passive response to pressure was determined in calcium-free solution containing EGTA (1 mmol/L). Data at each pressure were expressed as active diameter/maximum passive diameter (%D/D_{max}).

Drugs

Nifedipine, nimodipine, and mibefradil were from Sigma; efonidipine was kindly supplied by Nissan Chemical

Industries (Tokyo, Japan); and NNC 55-0396 was from Tocris Bioscience (Bristol, UK). Stock solutions (10 mmol/L) of nifedipine and nimodipine were dissolved in dimethyl sulfoxide and kept away from light to avoid photodegradation. Concentration ranges for drugs were chosen from previous studies that have used cells transfected with the relevant VDCC subtype or vascular preparations containing known VDCC subtypes (diltiazem, Feng and Navar, 2006; dihydropyridines, Furukawa *et al*, 2005; mibefradil, as reviewed by Heady *et al* (2001); NNC 55-0396, Huang *et al*, 2004). Therapeutic plasma levels of nimodipine achieved in clinical studies were within the range used in this study ($\sim 3 \mu\text{mol/L}$), although the concentration of nimodipine in cerebrospinal fluid was in the low nanomolar range.

Statistics

Activation and inactivation curves, including half maximal activation potentials ($V_{0.5}$) and slopes (k), were determined after normalization to maximal current and fit to Boltzmann equations. Time constants were derived from single- or double-exponential curves. Data were analysed using paired *t*-tests or two-way analysis of variance, followed by Bonferroni post-tests. A *P*-value less than 0.05 was considered significant.

Results

Expression of VDCC Subtypes

Semi-quantitative PCR showed that $\text{Ca}_v1.2$, 1.3, 2.1, 3.1, and 3.2 mRNA were expressed in both basilar arteries and MCAs and their branches. $\text{Ca}_v2.3$ was only detected in MCA vessels, whereas $\text{Ca}_v1.4$ was only detected in the MCA branch preparations (Supplementary Figure 1).

Using real-time PCR to quantify expression of $\text{Ca}_v1.2$, 1.3, 2.1, 3.1, and 3.2 mRNA, we found $\text{Ca}_v3.1$ and 1.2 to be the most highly expressed, being 5- to 10-fold higher than the other subtypes (Supplementary Table 1; $P < 0.05$). No significant difference in expression existed between arteries and their branches, except for $\text{Ca}_v3.2$, which showed lower expression in the basilar arteries and MCAs than in their branches, and $\text{Ca}_v2.1$, which showed higher expression in the basilar artery than in its branches.

Protein expression for each of $\text{Ca}_v1.2$, 1.3, 2.1, 3.1, and 3.2 was similar in both arteries and their branches. $\text{Ca}_v1.2$ was found in SMC membranes (Figures 1A-1C, arrow), but was absent from endothelial cells (ECs; Figures 1D and 1E). $\text{Ca}_v3.1$ was found in membranes and cytoplasm of SMCs and ECs (Figures 1G-1K). $\text{Ca}_v3.2$ staining was similar to $\text{Ca}_v3.1$ (Figures 1M-1Q). In contrast, $\text{Ca}_v2.3$ was confined to the adventitia where it appeared to be localized to nerve fibres (Supplementary Figure 2). For each of these antibodies, staining was abolished after incubation with antigenic peptide (Figures 1F, 1L, and 1R). Staining with antibodies against $\text{Ca}_v1.3$

and 2.1 was not abolished by this procedure and therefore was considered to be nonspecific.

High-pressure freezing, freeze-substitution, and low-temperature embedding enabled good ultrastructural tissue preservation (Figure 2A). Immunostaining showed $\text{Ca}_v1.2$ and 3.1 localized within the cytoplasm and membranes of SMCs (Figures 2B-2G, panels a, d, and e), without any significant high-resolution colocalization (Figures 2F and 2G). Staining for $\text{Ca}_v3.1$, but not for $\text{Ca}_v1.2$, was found in the cytoplasm and membranes of ECs (Figure 2D, panels b and c). Specificity of labelling was shown because staining was abolished by preincubation in antibody with an excess of the immunizing peptide (Figures 2B, inset; Figures 2E, inset). Under these conditions, gold particle density was ~ 100 -fold lower and comparable to that over SMC or EC nuclei (nu), internal elastic lamina (IEL), vessel lumen or adventitia (adv), where gold particles were rare (Figures 2B-2G).

Voltage-Dependent Calcium Currents in Isolated SMCs

Isolated SMCs were spindle shaped and protein expression was assessed by immunohistochemistry for $\text{Ca}_v1.2$ and 3.1, immediately after dissociation and at the end of patch clamp experiments (5 h after isolation). Staining suggested that $\text{Ca}_v1.2$ and 3.1 protein distribution was not adversely affected by the cell isolation procedure (Figure 3A). $\text{Ca}_v3.2$ was more weakly expressed.

High-voltage-activated calcium currents were evoked from holding potentials of -100 , -70 , or -50 mV, with 10 mmol/L Ba^{2+} as charge carrier (Figures 3B-3E). These potentials were chosen to maximally evoke T-type currents (-100 mV) and to emulate the resting membrane potential in fully relaxed, unpressurized vessels (-70 mV) or myogenically active vessels (-50 mV, Knot and Nelson, 1998). No significant differences were found in the half-maximal activation potentials ($V_{0.5}$) or slopes (k) of activation among the holding potentials (Figures 3C-3E; Supplementary Table 2), although currents tended to be larger when evoked from more negative potentials (Figure 3C). Inactivation characteristics were also similar (Figure 3E).

Currents had similar biophysical characteristics irrespective of the arterial origin of the SMCs (Supplementary Table 2). Replacement of Ba^{2+} with 2 mmol/L Ca^{2+} as charge carrier caused a shift to more negative activation potentials and decreased activation and inactivation time constants (Supplementary Table 2), as reported previously (Shcheglovitov *et al*, 2007).

Effect of L-Channel Blockers on Calcium Currents

Nifedipine ($1 \mu\text{mol/L}$) reduced inward currents in SMCs isolated from the main basilar artery to $12\% \pm 2.4\%$ of the current in control solution when

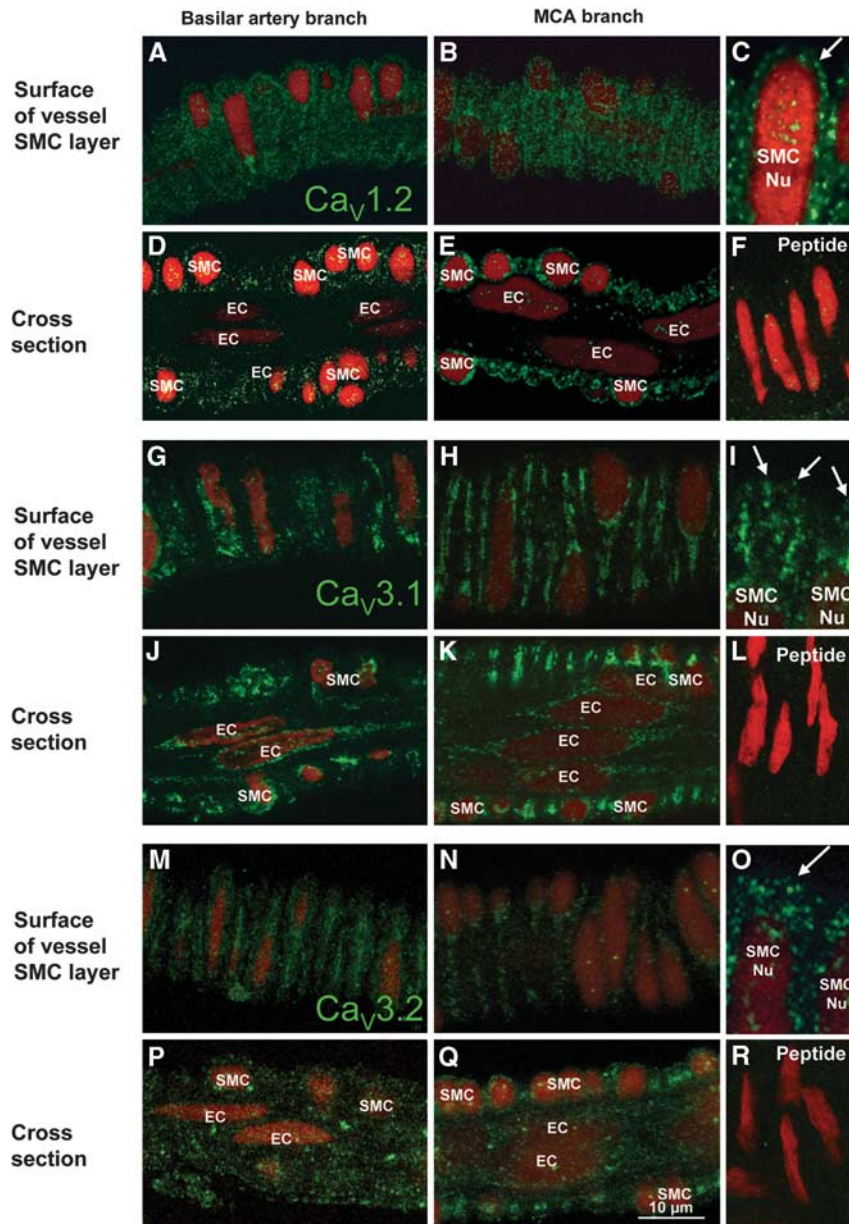


Figure 1 Distribution of L- and T-type channels in basilar and middle cerebral arteries. (A–F) L-type channels ($Ca_v1.2$) are expressed in membranes of SMCs (A–C, arrow) but not endothelial cells (ECs; D, E). Staining of $Ca_v1.2$ is blocked with the immunogenic peptide (F). (G–L) T-type channels ($Ca_v3.1$) are expressed in cytoplasm and membranes (arrows) of SMCs (G–I, arrow) and ECs (J, K). Staining is abolished after incubation with immunogenic peptide (L). (M–R) $Ca_v3.2$ channels are expressed in SMCs (M–O) and ECs (P, Q) similar to $Ca_v3.1$. Staining is abolished after incubation with immunogenic peptide (R). Nuclei (Nu) are stained with propidium iodide (red). Images in C, I, and O are higher power magnifications of MCA VDCC staining. The longitudinal vessel axis is left to right in all panels. Staining is indicative of at least four preparations.

tested from a holding potential of -50 mV, to $22\% \pm 3.1\%$ of control current from -70 mV, and to $30\% \pm 7.6\%$ of control current from -100 mV (Figures 4A and 4B, Supplementary Table 3). As the residual current from -50 mV was small, the subsequent analysis was confined to currents evoked from -70 and -100 mV. Effects of nifedipine were not time dependent as there was no change in evoked current during repetitive depolarizing protocols from -70 to $+10$ mV (Figure 4C).

The nifedipine-insensitive component showed significant changes in biophysical characteristics from the nifedipine-sensitive current. $V_{0.5}$ was significantly shifted to more negative potentials (-8.9 ± 1.8 to -12.5 ± 1.4 mV, from -70 mV), without any change in k , whereas time constants for activation and inactivation of the nifedipine-insensitive current were significantly faster than those for the nifedipine-sensitive component (Figures 4D–4F; Supplementary Table 3). In contrast, time constants for

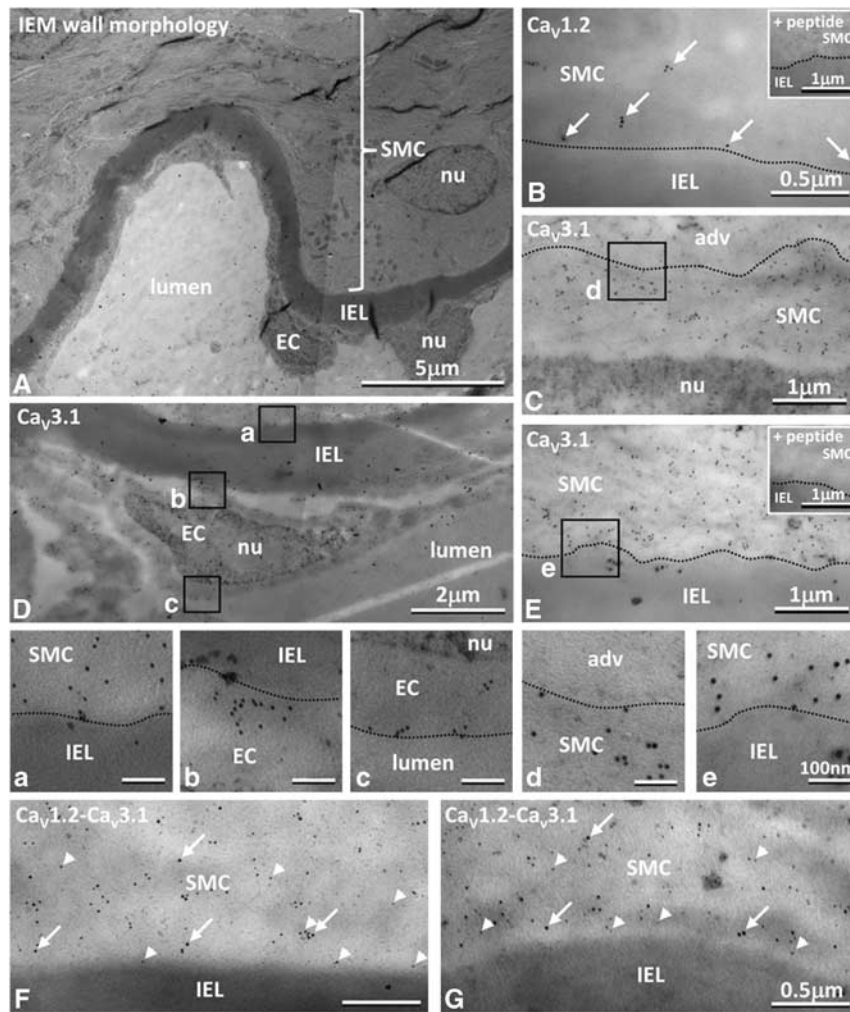


Figure 2 Location of L- and T-type channels at the ultrastructural level. **(A)** Tissue prepared for immunoelectron microscopy shows normal vessel morphology with smooth muscle cells (SMCs) and endothelial cells (ECs) separated by the internal elastic lamina (IEL); with myosin filaments oriented to the longitudinal cell axis and accumulations of mitochondria within the cells. **(B–G)** Gold labelled $Ca_v1.2$ (10 nm) and $Ca_v3.1$ (5 nm) were found in the SMC cytoplasm and at cell membranes **(B, C, E–G)**. $Ca_v3.1$ was also found in ECs **(D)**. Boxes in **C–E** shown at higher magnification in panels a–e. Gold particles were rarely found over nuclei (nu: **C, D**, panel c), adventitia (adv: **C**, panel d), IEL (**B, E**, panels a, b, and e, **F, G**), or lumen (panel c), and staining was abolished after incubation with appropriate corresponding immunogenic peptide (insets in **B, E**).

deactivation were significantly increased compared to control (Figures 4G and 4H).

A lower concentration of nifedipine (0.1 $\mu\text{mol/L}$) produced a larger nifedipine-resistant component in the basilar artery (70% \pm 11% of control current), but there was no longer any significant change in time course (Supplementary Table 3), suggesting an incomplete block of the L-type channels.

Significantly larger nifedipine-insensitive currents were evoked from SMCs isolated from arterial branches than from the main basilar artery (33% \pm 8% of control current from -50 mV , 47% \pm 7% of control current from -70 mV ; Figure 6B, Supplementary Table 3), although the overall currents in these SMCs were smaller (max current of 90 pA). Nevertheless, from a holding potential of -70 mV , the activation and inactivation time courses were again significantly

faster and $V_{0.5}$ shifted to more negative potentials (Supplementary Table 3).

Nimodipine (10 $\mu\text{mol/L}$) produced results similar to nifedipine on currents evoked from -70 mV in basilar artery SMCs, with 24% \pm 5% of control current remaining. This insensitive current exhibited a significant leftward shift in $V_{0.5}$ and significantly faster activation and inactivation time constants (Figures 5A, 5B, and 5D; Supplementary Table 3). A lower concentration of nimodipine (1 $\mu\text{mol/L}$) resulted in a larger resistant component (36% \pm 10% of control current) with similar changes in time course (Supplementary Table 3).

Inactivation curves for both the nifedipine- and nimodipine-insensitive currents were significantly shifted to more negative potentials leading to a left-shifted persistent window current (Figures 5C and 5D).

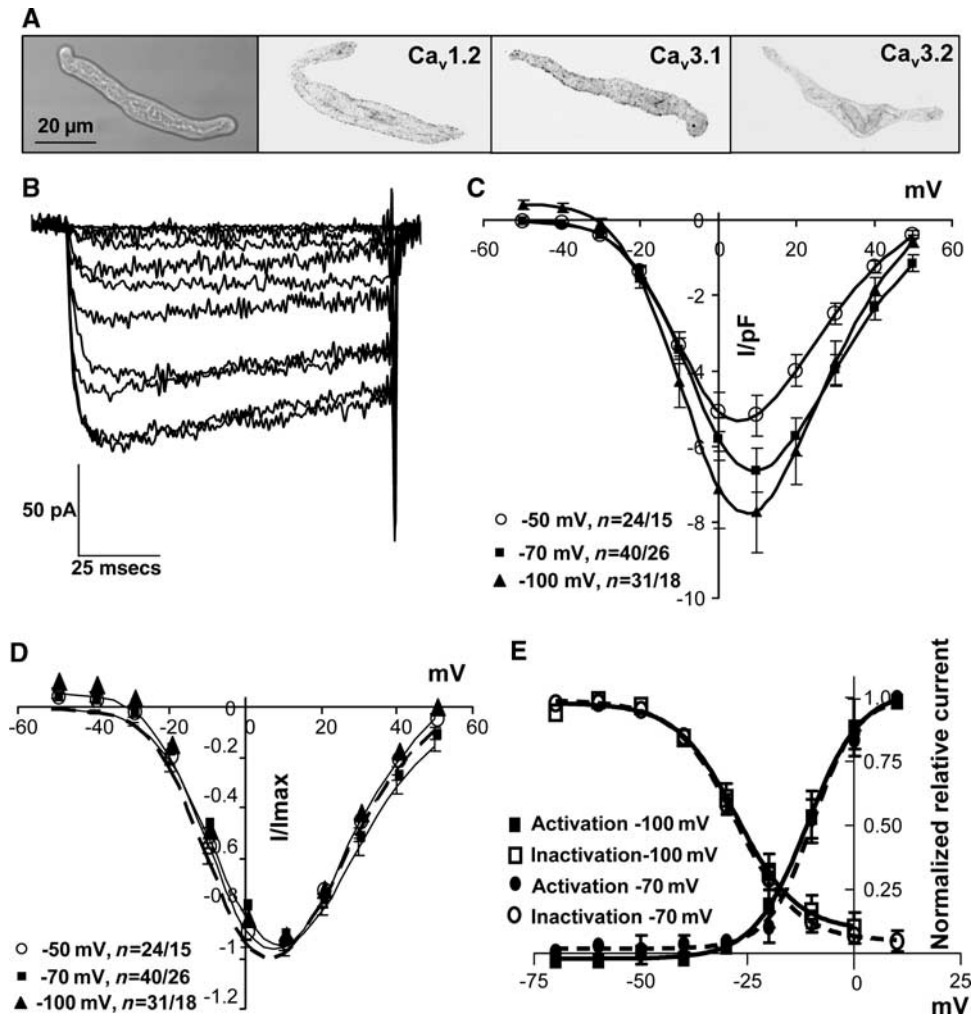


Figure 3 Voltage-dependent calcium currents in cerebrovascular SMCs. (A) Isolated SMCs were spindle-shaped and expressed L- and T-type channels ($Ca_v1.2$ and 3.1) with reduced $Ca_v3.2$ expression. Immunohistochemistry images were converted to black on white. (B) Ba^{2+} currents evoked from a holding potential of -70 mV with incremental 10 mV depolarizing steps between -50 and $+50$ mV. (C, D) Group data for currents evoked from -50 , -70 , and -100 mV, normalized to cell capacitance (C) or peak current (D). (E) Activation and inactivation curves from -70 and -100 mV. n = number of cells/animals.

To confirm that the nifedipine-resistant component was not an L-type current with reduced dihydropyridine sensitivity, we tested the non-dihydropyridine blocker, diltiazem ($10 \mu\text{mol/L}$) on the left-shifted nifedipine-insensitive current. No further reduction in the residual current or alteration in its characteristics was seen in the combined presence of nifedipine and diltiazem (Figures 5E and 5F; Supplementary Table 3).

Data showed that non-L-type calcium currents, with activation and inactivation curves shifted to more negative potentials and significantly faster time courses than L-type currents, were evoked by voltage in cerebrovascular SMCs.

Effect of T-Channel Blockers on Calcium Currents

Mibefradil ($1 \mu\text{mol/L}$) abolished the nimodipine- and nifedipine-insensitive calcium currents in SMCs from the main basilar artery (Figures 5A, 5B, and

6A) and side branches, although $3 \mu\text{mol/L}$ mibefradil was required in the latter (Figure 6B). In the absence of nifedipine or nimodipine, mibefradil abolished all current (Figures 6C and 6D). NNC 55-0396 ($1 \mu\text{mol/L}$), a mibefradil analogue, reported to be without effects on L-type channels in expression systems at concentrations below $100 \mu\text{mol/L}$ (Huang *et al*, 2004; Li *et al*, 2005), also abolished all current (Figures 6E and 6F), as did the dual L- and T-type blocker, efonidipine ($10 \mu\text{mol/L}$). None of the T-type antagonists were reversible.

These data showed that putative T-type blockers also inhibit evoked L-type currents in cerebrovascular SMCs.

Effect of L- and T-Type Blockers on Pressure-Induced Constriction and Tone

The main basilar artery and its larger and smaller branches showed pressure-dependent constrictions

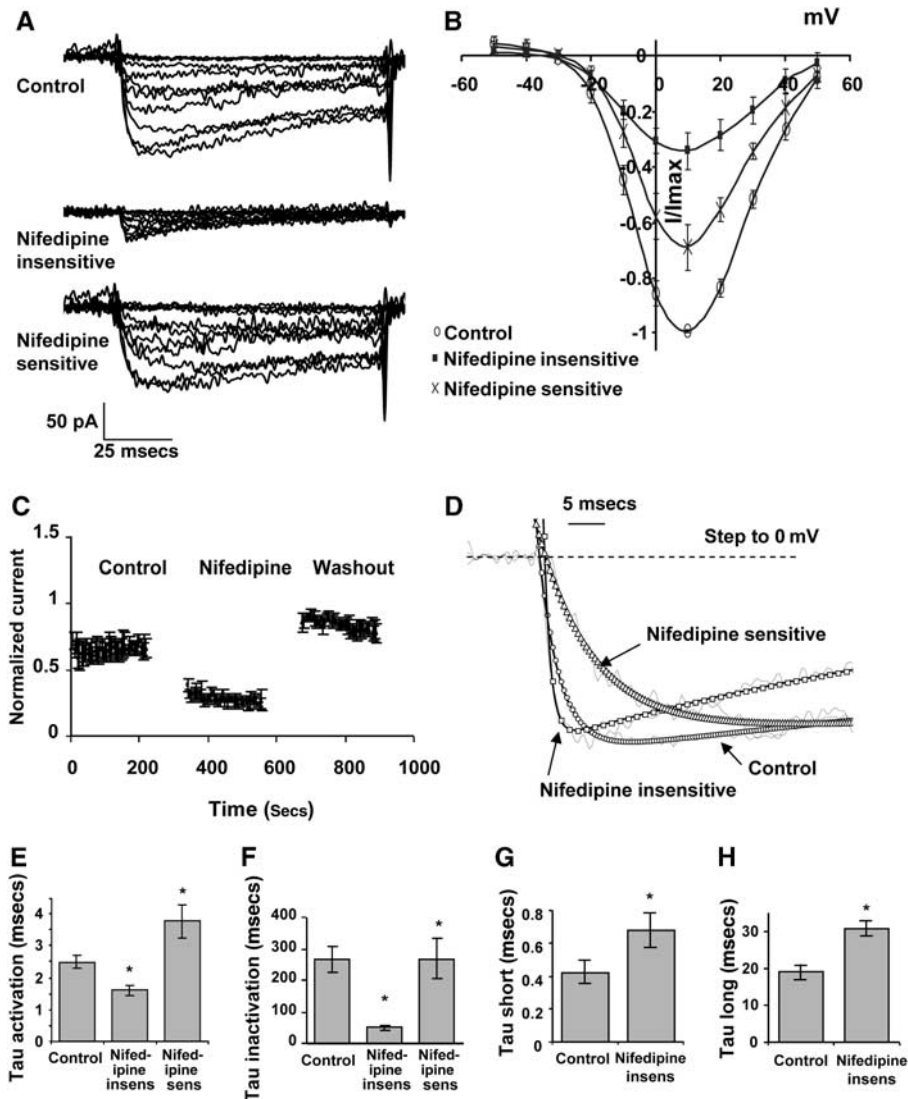


Figure 4 Effect of nifedipine on calcium currents. (A) Calcium currents evoked from holding potential of -70 mV were reduced by nifedipine ($1 \mu\text{mol/L}$) and restored on wash out. (B) Group data of nifedipine-sensitive and insensitive currents, $n = 8$ cells. (C) Effects of nifedipine did not increase with time of application to current evoked by repetitive depolarizing steps from -70 to $+10$ mV, $n = 4$ cells. (D–F) Nifedipine-insensitive currents had significantly faster activation (D, E) and inactivation time constants (D, F). Traces in D have been normalized to maximum current evoked with a depolarizing step to 0 mV from a holding potential of -70 mV. (G, H) Nifedipine-insensitive tail currents were fitted with two time constants that were both significantly slower than control, $n = 9$ cells. $*P < 0.05$ significantly different from paired control.

that were abolished in the absence of calcium (Figures 7A, 7B, and 7C, respectively). Although pressure-induced constriction in the main basilar artery was abolished by nifedipine ($1 \mu\text{mol/L}$; Figure 7A), the same concentration did not completely abolish constriction in the larger branches (Figure 7B) and only partially inhibited the pressure-dependent myogenic constrictions at pressures > 60 mm Hg in the smaller branches (Figure 7C). Tone was inhibited further when mibefradil (1 or $3 \mu\text{mol/L}$) was added together with nifedipine (Figures 7B and 7C).

In the large branches, in comparison with nifedipine alone that only partially reduced constriction (Figure 7D), mibefradil was found to nearly abolish

constriction at $1 \mu\text{mol/L}$, suggesting a combined action on L- and T-type channels, whereas at $10 \mu\text{mol/L}$ it produced constriction (Figure 7E). This latter effect is likely to be due to action on potassium channels, because it was reduced after pretreatment with tetraethylammonium (data not shown). A more selective analogue of mibefradil, NNC 55-0396, produced a concentration-dependent inhibition of constriction (although, unlike mibefradil, it did not produce constriction) that was inhibited further by nifedipine (Figure 7F).

In summary, pressure-induced vasoconstrictions in the main basilar artery were completely dependent on L-type channels, whereas in the large and small side branches, an increasingly large compo-

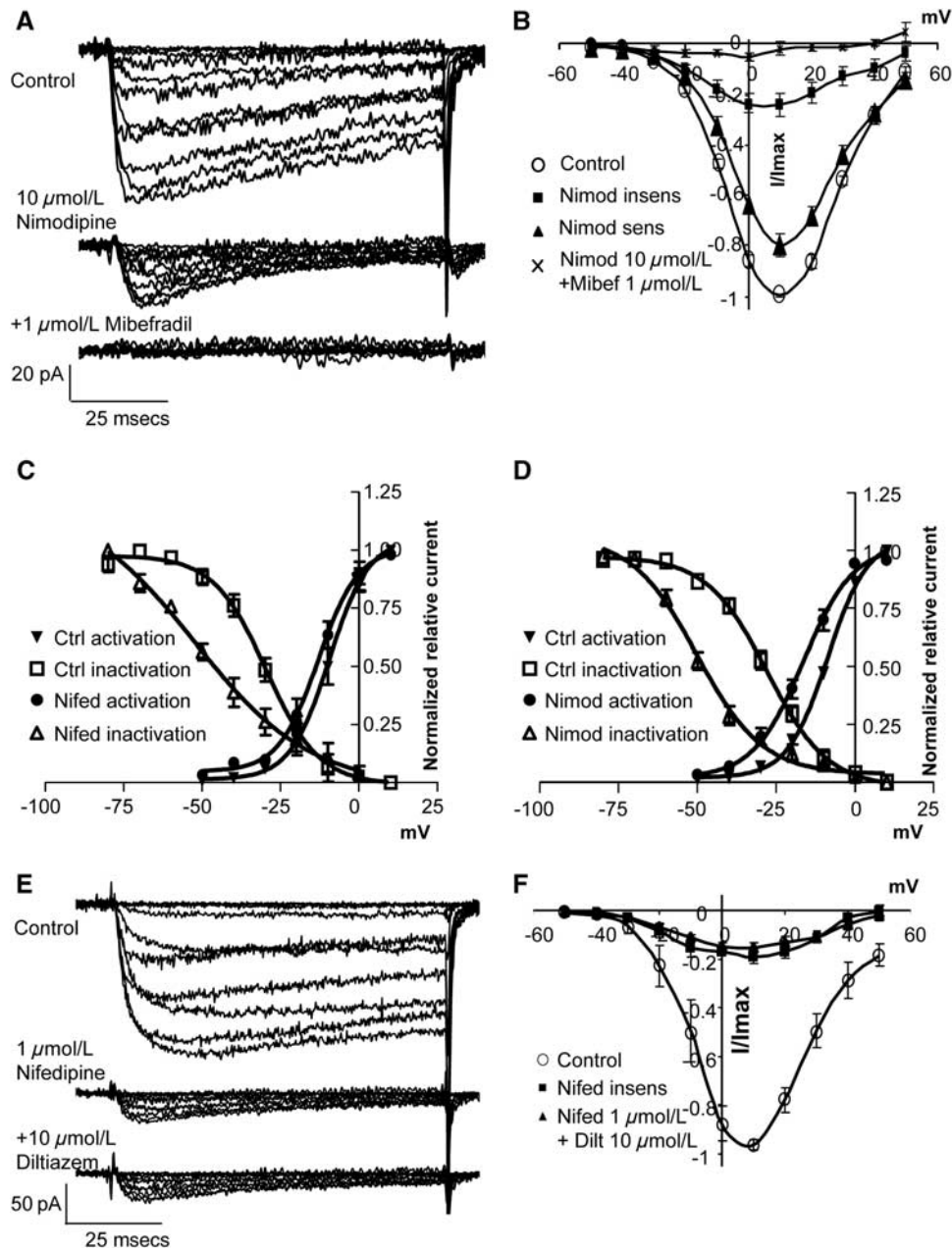


Figure 5 Effect of L-type blockers on calcium currents. **(A)** Calcium currents evoked from holding potential of -70 mV were reduced by nimodipine ($10 \mu\text{mol/L}$) and abolished by addition of mibefradil ($1 \mu\text{mol/L}$). **(B)** Group data $n = 10$ cells. **(C, D)** After inhibition of L-type currents with nifedipine **(C)** or nimodipine **(D)**, window currents were left shifted due to a significant change in the activation and inactivation curves of the dihydropyridine-resistant current (see Supplementary Table 3 for details). **(E)** Calcium currents evoked from holding potential of -70 mV were reduced by nifedipine ($1 \mu\text{mol/L}$), but not affected by addition of diltiazem ($10 \mu\text{mol/L}$). **(F)** Group data $n = 4$ cells.

ment of tone was resistant to block with nifedipine; resistance being the greatest in the smaller vessels.

Discussion

This study shows for the first time that a heterogeneous population of dihydropyridine-sensitive and insensitive VDCCs contributes to vasoconstriction of small cerebral arteries; the dihydropyridine-

insensitive channels having a more prominent role as vessel size decreases. Moreover, in SMCs isolated from either basilar artery or MCA, a high-voltage-activated calcium current, which was insensitive to the dihydropyridines, nifedipine, and nimodipine, was also found and this current could be completely blocked with the putative T-type channel blockers, mibefradil, NNC 55-0396, and efonidipine. Although the dihydropyridine-sensitive component of the current exhibited biophysical

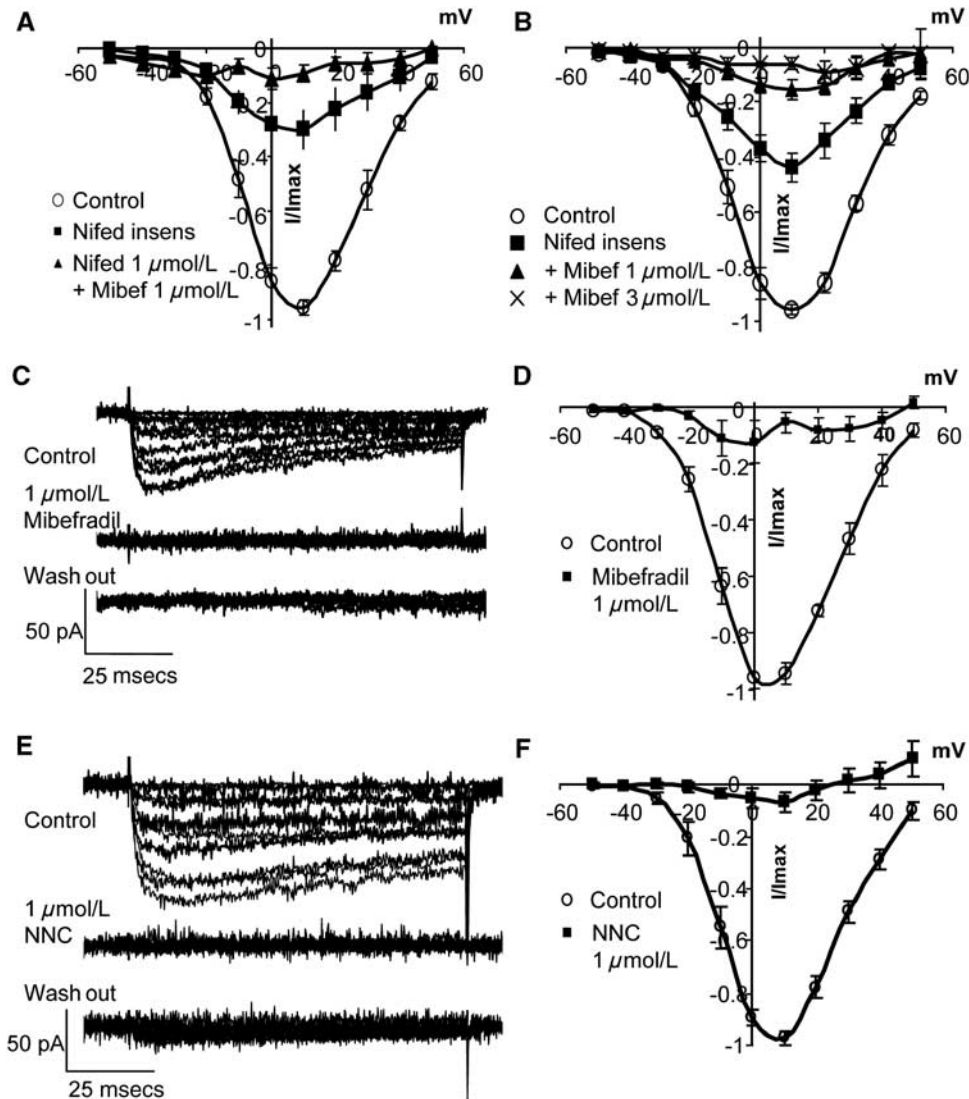


Figure 6 Effect of L- and T-type blockers on calcium currents. (A) Calcium currents in SMCs from the main basilar artery, evoked from holding potential of -70 mV, were reduced by nifedipine ($1 \mu\text{mol/L}$) and abolished by addition of mibefradil ($1 \mu\text{mol/L}$; $n = 4$ cells). (B) In SMCs from basilar side branches, there was a larger nifedipine-insensitive component ($1 \mu\text{mol/L}$) that was abolished with mibefradil (1, 3 $\mu\text{mol/L}$; $n = 9$ cells). (C–F) T-type blockers, mibefradil ($1 \mu\text{mol/L}$), and NNC 55-0396 ($1 \mu\text{mol/L}$) blocked all evoked current in SMCs from the main basilar artery. (D, F) Group data $n = 4$ cells.

characteristics typical of L-type VDCCs, the activation and inactivation characteristics of the insensitive current were significantly faster, the deactivation time course significantly slower, and the persistent window current shifted to more hyperpolarized potentials. The greater contribution of these dihydropyridine-insensitive currents to evoked calcium currents of SMCs and to pressure-induced vasoconstriction of smaller cerebral arteries suggests that they have a significant function in cerebrovascular resistance.

While myogenic constriction of pressurized main basilar arteries was abolished by nifedipine, consistent with earlier observations reported in the larger rat posterior cerebral arteries (Knot and Nelson, 1998), a significant component was resistant in smaller diameter side branches. The smaller calibre

vessel data are in accordance with the finding that a greater proportion of the evoked calcium current in SMCs isolated from branches of the basilar artery was dihydropyridine-resistant, compared with that in SMCs from the main basilar artery. Interestingly, a high-voltage-activated nifedipine-insensitive current was also more prominent in smaller mesenteric arterioles (Morita *et al*, 1999; Morita *et al*, 2002). In the smaller side branches of our study, nifedipine only partially inhibited myogenic vasoconstriction and only at pressures greater than 60 mmHg, indicating that conventional dihydropyridine-resistant L-type channels have a minor role in maintaining tone of these smaller arteries. This observation corroborates our recently published findings that showed abolition of vasomotion by nifedipine in small basilar side branches taken from juvenile rats,

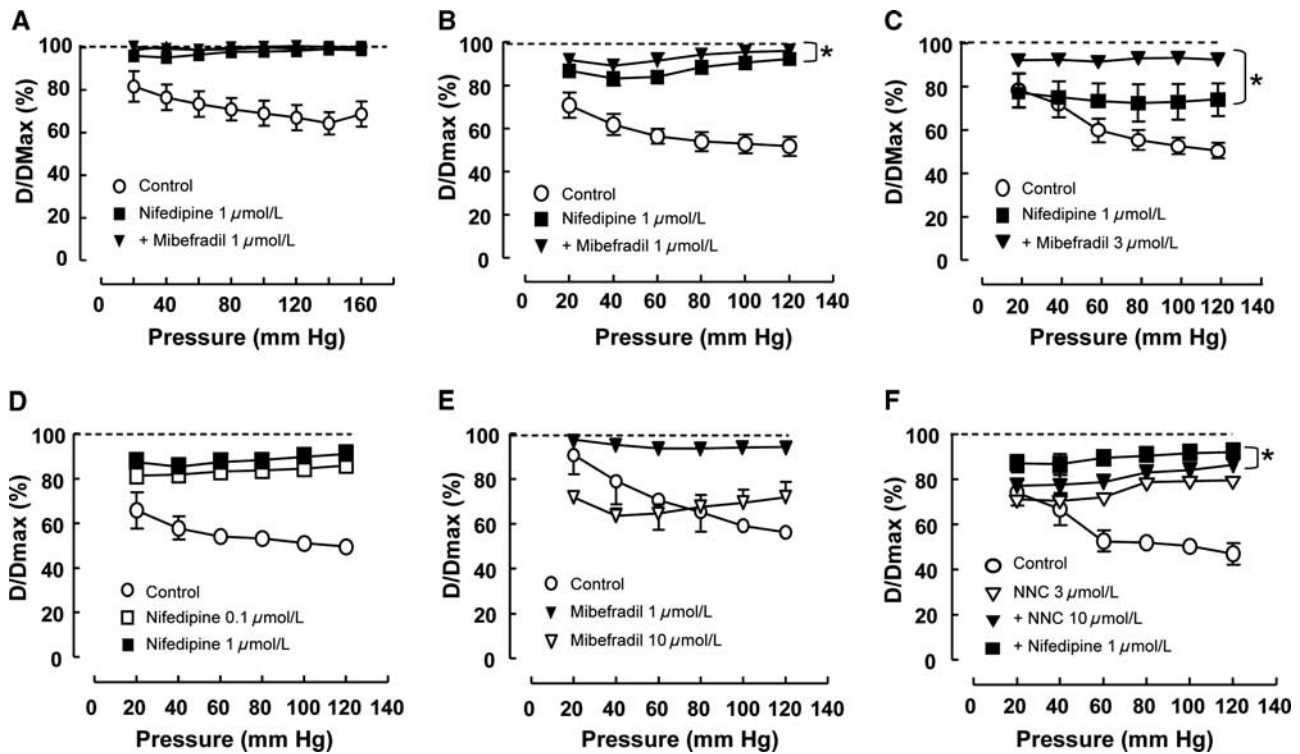


Figure 7 Effect of L- and T-type blockers on myogenic tone of basilar artery (A) and branches (B–F). (A–C) Nifedipine-resistant tone increased with decreasing vessel size. In the main basilar artery (vessel diameter 319 μm), nifedipine (1 μmol/L) completely abolished vascular tone, and mibefradil (1 μmol/L) had no additional effect (A). In the larger branches (vessel diameter 172 μm), addition of mibefradil (1 μmol/L) after nifedipine (1 μmol/L) caused a further significant relaxation (B). In the smaller side branches (vessel diameter 101 μm), nifedipine (1 μmol/L) only partially reduced tone at pressures above 60 mm Hg and addition of mibefradil (3 μmol/L) significantly reduced tone at all pressures (C). (D–F) Effects of L- and T-type blockers in the larger branches of the basilar artery. Nifedipine (0.1, 1 μmol/L) caused a dose-dependent relaxation, but did not completely abolish tone (D). Mibefradil alone inhibited constriction at 1 μmol/L, but induced constriction at 10 μmol/L (E). The T-type blocker, NNC 55-0396, caused a dose-dependent inhibition of constriction that was further inhibited by the addition of nifedipine (1 μmol/L) (F). **P* < 0.05, two-way analysis of variance, *n* = 4 to 6 vessels.

but without any corresponding inhibition of tone (Navarro-Gonzalez *et al*, 2009). The persistence in $Ca_v1.2$ knockout mice of myogenic constriction in skeletal muscle arteries in response to pressures up to 40 mmHg (Moosmang *et al*, 2003) is consistent with the shift we see in window current to more negative potentials after treatment with dihydropyridines, and indicative of a more prominent effect at lower systemic pressures where membrane potential is more hyperpolarized (Knot and Nelson, 1998).

Both L- ($Ca_v1.2$) and T-type ($Ca_v3.1$ and 3.2) channels were the major VDCC subtypes expressed in SMCs of the MCAs and basilar arteries at both mRNA and protein levels. This distribution is consistent with our previous studies in juvenile rats (Navarro-Gonzalez *et al*, 2009) and with studies in other vascular beds (Hansen *et al*, 2001; Jensen *et al*, 2004; Morita *et al*, 2002; VanBavel *et al*, 2002); however, the expression of $Ca_v3.1$ and 3.3, but not $Ca_v3.2$, in the dog basilar artery is suggestive of species variation (Nikitina *et al*, 2007). In this study, $Ca_v3.1$ and 3.2 were also detected in ECs, although a function for VDCCs in the endothelium is yet to be established. Nevertheless, the recent demonstration

in mesenteric arterioles of $Ca_v3.2$ protein in ECs (Braunstein *et al*, 2008) may suggest a more widespread distribution in this cell layer. Although considerable expression for the T-type channels was found in the cytoplasm of SMCs, our ultrastructural studies showed that $Ca_v3.1$ protein, similar to that of $Ca_v1.2$, could be found at the cell membrane. However, we did not find any evidence for high-resolution colocalization of L- and T-type channels, as has been suggested recently to account for overlapping pharmacological actions of L- and T-type antagonists in mesenteric arterioles (Braunstein *et al*, 2008).

In spite of the expression of T-type channels, we did not find any evidence for low-voltage-activated currents in cerebrovascular SMCs, although low-voltage-activated currents, sensitive to both nimodipine and mibefradil, have been recorded in SMCs from dog basilar arteries (Nikitina *et al*, 2007). However, we did find that ~20% of the calcium current recorded in isolated SMCs persisted in the presence of either nifedipine (1 μmol/L) or nimodipine (10 μmol/L) and that this resistant component displayed biophysical characteristics more similar to

that of a T-type current. The lack of a significant effect of a lower concentration of nifedipine (0.1 $\mu\text{mol/L}$) on the biophysical parameters of the residual current suggests that this concentration produced an incomplete block of L-type channels. This contrasts with the appreciably lower IC_{50} for nifedipine determined in cell lines transfected with $\text{Ca}_v1.2$ channels (Lee *et al*, 2006), raising the question of whether pharmacological data obtained in transfected cell lines are applicable to channel function of native SMCs.

The present single cell data confirm that mibefradil, as well as the more selective T-type blockers, NNC and efonidipine, block L-type VDCCs, as well as dihydropyridine-insensitive channels. However, the persistence of a small L-type component of the myogenic response in pressurized cerebral arteries in the presence of NNC may indicate that isolated SMCs do not behave exactly as they do in their normal cellular environment. Alternatively, we cannot rule out the possibility that the use of barium as charge carrier in the isolated SMCs could have increased the sensitivity of the native L-type channels to T-type channel blockers. Nevertheless, the results indicate that caution should be exercised when using these putative T-type blockers to define a contribution of T-type channels in tissue preparations.

Pressure-evoked vasoconstriction and vasomotion of cerebral vessels has previously been shown to depend on the activity of transient receptor potential channels that provide the depolarization required to activate the VDCCs studied here (Brayden *et al*, 2008; Wolfle *et al*, 2010). L-type VDCCs also interact closely with ryanodine receptors and large conductance calcium-activated potassium channels to provide a negative feedback on cerebral vasoconstriction (Jaggar *et al*, 1998). Our preliminary data of attenuation by the nonselective potassium channel antagonist, tetraethylammonium, of the anomalous constriction induced by high concentrations of mibefradil may suggest that the dihydropyridine-insensitive VDCCs described here also form spatially close relationships with potassium channels. Further investigation of these potential interactions is warranted.

In view of the data presented here, the question arises as to the molecular identity of the dihydropyridine-insensitive current. Recent studies indicate that the genes encoding L-type VDCCs undergo significant splice variation producing channels that activate at more hyperpolarized potentials (Cheng *et al*, 2009; Liao *et al*, 2007). However, the current described in this study differs from these L-type splice variants in several ways. First, it is insensitive to nifedipine and nimodipine, whereas the L-type variants are more sensitive to dihydropyridines (Liao *et al*, 2007). Interestingly, an L-type splice variant found in the rat heart has been reported to be less sensitive to the dihydropyridine nisoldipine, although this variant was not detected in vascular smooth muscle (Welling *et al*, 1997). Second, the

inactivation time course of the nifedipine-insensitive component described here was similar to that of a T-type channel (Perez-Reyes, 2003) and considerably faster than the L-type splice variants (Cheng *et al*, 2009; Liao *et al*, 2007). Third, the tail currents of the nifedipine-resistant component were significantly slower than the composite current, again being similar to T-type channels that undergo slower deactivation (Lacinova, 2005; Perez-Reyes, 2003) than L-type channels (Brown *et al*, 1993). Finally, no further attenuation of the nifedipine-insensitive current was observed after addition of the benzothiazepine, diltiazem, indicating that the concentration of nifedipine used was sufficient to completely block L-type currents. Conversely, the similarity in time course of the nifedipine-insensitive component to T-type channels suggests that the current may arise from a T-channel splice variant. T-type channel splice variants have been described to alter surface expression (Shcheglovitov *et al*, 2008), as well as to shift activation to more positive potentials (Chemin *et al*, 2001; Emerick *et al*, 2006). Of further interest is the reduced sensitivity to mibefradil of the channels in the smaller branches. However, we did not find any evidence for a low-voltage-activated current that is a diagnostic feature of T-type channel activity. Thus, to summarize, the current recorded in this study has the pharmacological and biophysical characteristics of a T-type channel with the voltage sensitivity of an L-type channel. Clearly, a complete molecular biological and pharmacological analysis is required to resolve this issue.

In conclusion, the present data provide evidence for a population of dihydropyridine-insensitive VDCCs that contribute to vascular tone of small cerebral vessels. Although both L- and T-type channels are highly expressed in these vessels, the precise molecular identity of these dihydropyridine-insensitive channels is currently uncertain. Nevertheless, the responsiveness of these channels to nonselective T-type VDCC blockers suggests that these drugs may well provide a more effective treatment for therapy-resistant vasospastic conditions of the cerebral circulation.

Acknowledgements

We thank Dr M Louise Tierney for patch clamp equipment and advice.

Conflict of interest

The authors declare no conflict of interest.

References

- Ball CJ, Wilson DP, Turner SP, Saint DA, Beltrame JF (2009) Heterogeneity of L- and T-channels in the vasculature:

- rationale for the efficacy of combined L- and T-blockade. *Hypertension* 53:654–60
- Baylis C, Qiu C, Engels K (2001) Comparison of L-type and mixed L- and T-type calcium channel blockers on kidney injury caused by deoxycorticosterone-salt hypertension in rats. *Am J Kidney Dis* 38:1292–7
- Beltrame JF, Turner SP, Leslie SL, Solomon P, Freedman SB, Horowitz JD (2004) The angiographic and clinical benefits of mibefradil in the coronary slow flow phenomenon. *J Am Coll Cardiol* 44:57–62
- Braunstein TH, Inoue R, Cribbs L, Oike M, Ito Y, Holstein-Rathlou NH, Jensen LJ (2008) The role of L- and T-type calcium channels in local and remote calcium responses in rat mesenteric terminal arterioles. *J Vasc Res* 46:138–51
- Brayden JE, Earley S, Nelson MT, Reading S (2008) Transient receptor potential (TRP) channels, vascular tone and autoregulation of cerebral blood flow. *Clin Exp Pharmacol Physiol* 35:1116–20
- Brown AM, Schwandt PC, Crill WE (1993) Voltage dependence and activation kinetics of pharmacologically defined components of the high-threshold calcium current in rat neocortical neurons. *J Neurophysiol* 70:1530–43
- Chemin J, Monteil A, Bourinet E, Nargeot J, Lory P (2001) Alternatively spliced alpha(1G) (Ca_v3.1) intracellular loops promote specific T-type Ca²⁺ channel gating properties. *Biophys J* 80:1238–50
- Cheng X, Pachauu J, Blaskova E, Asuncion-Chin M, Liu J, Dopico AM, Jaggar JH (2009) Alternative splicing of Cav1.2 channel exons in smooth muscle cells of resistance-size arteries generates currents with unique electrophysiological properties. *Am J Physiol Heart Circ Physiol* 297:H680–8
- Clozel JP, Ertel EA, Ertel SI (1997) Discovery and main pharmacological properties of mibefradil (Ro 40-5967), the first selective T-type calcium channel blocker. *J Hypertens Suppl* 15:S17–25
- Dorhout Mees SM, Rinkel GJ, Feigin VL, Algra A, van den Bergh WM, Vermeulen M, van Gijn J (2007) Calcium antagonists for aneurysmal subarachnoid haemorrhage. *Cochrane Database Syst Rev* 34:CD000277
- Emerick MC, Stein R, Kunze R, McNulty MM, Regan MR, Hanck DA, Agnew WS (2006) Profiling the array of Ca_v3.1 variants from the human T-type calcium channel gene CACNA1G: alternative structures, developmental expression, and biophysical variations. *Proteins* 64:320–42
- Ertel SI, Ertel EA, Clozel JP (1997) T-type Ca²⁺ channels and pharmacological blockade: potential pathophysiological relevance. *Cardiovasc Drugs Ther* 11:723–39
- Feng MG, Navar LG (2006) Nitric oxide synthase inhibition activates L- and T-type Ca²⁺ channels in afferent and efferent arterioles. *Am J Physiol Renal Physiol* 290:F873–9
- Furukawa T, Miura R, Honda M, Kamiya N, Mori Y, Takeshita S, Isshiki T, Nukada T (2004) Identification of R(-)-isomer of efonidipine as a selective blocker of T-type Ca²⁺ channels. *Br J Pharmacol* 143:1050–7
- Furukawa T, Nukada T, Miura R, Ooga K, Honda M, Watanabe S, Koganesawa S, Isshiki T (2005) Differential blocking action of dihydropyridine Ca²⁺ antagonists on a T-type Ca²⁺ channel (alpha1G) expressed in *Xenopus oocytes*. *J Cardiovasc Pharmacol* 45:241–6
- Gustafsson F, Andreassen D, Salomonsson M, Jensen BL, Holstein-Rathlou N (2001) Conducted vasoconstriction in rat mesenteric arterioles: role for dihydropyridine-insensitive Ca²⁺ channels. *Am J Physiol Heart Circ Physiol* 280:H582–90
- Haddock RE, Grayson TH, Brackenbury TD, Meaney KR, Neylon CB, Sandow SL, Hill CE (2006) Endothelial coordination of cerebral vasomotion via myoendothelial gap junctions containing connexins 37 and 40. *Am J Physiol Heart Circ Physiol* 291:H2047–56
- Hansen PB, Jensen BL, Andreassen D, Skott O (2001) Differential expression of T- and L-type voltage-dependent calcium channels in renal resistance vessels. *Circ Res* 89:630–8
- Heady TN, Gomora JC, Macdonald TL, Perez-Reyes E (2001) Molecular pharmacology of T-type Ca²⁺ channels. *Jpn J Pharmacol* 85:339–50
- Huang L, Keyser BM, Tagmose TM, Hansen JB, Taylor JT, Zhuang H, Zhang M, Ragsdale DS, Li M (2004) NNC 55-0396 [(1S,2S)-2-(2-(N-[(3-benzimidazol-2-yl)propyl]-N-methylamino)ethyl)-6-fluoro-1,2,3,4-tetrahydro-1-isopropyl-2-naphthyl cyclopropanecarboxylate dihydrochloride]: a new selective inhibitor of T-type calcium channels. *J Pharmacol Exp Ther* 309:193–9
- Jaggar JH, Wellman GC, Heppner TJ, Porter VA, Perez GJ, Gollasch M, Kleppisch T, Rubart M, Stevenson J, Lederer WJ, Knot HJ, Bonev AD, Nelson MT (1998) Ca²⁺ channels, ryanodine receptors and Ca²⁺-activated K⁺ channels: a functional unit for regulating arterial tone. *Acta Physiol Scand* 164:577–87
- Jensen LJ, Salomonsson M, Jensen BL, Holstein-Rathlou NH (2004) Depolarization-induced calcium influx in rat mesenteric small arterioles is mediated exclusively via mibefradil-sensitive calcium channels. *Br J Pharmacol* 142:709–18
- Knot HJ, Nelson MT (1998) Regulation of arterial diameter and wall [Ca²⁺] in cerebral arteries of rat by membrane potential and intravascular pressure. *J Physiol* 508:199–209
- Lacinova L (2005) Voltage-dependent calcium channels. *Gen Physiol Biophys* 24(Suppl 1):1–78
- Lee TS, Kaku T, Takebayashi S, Uchino T, Miyamoto S, Hadama T, Perez-Reyes E, Ono K (2006) Actions of mibefradil, efonidipine and nifedipine block of recombinant T- and L-type Ca channels with distinct inhibitory mechanisms. *Pharmacology* 78:11–20
- Li M, Hansen JB, Huang L, Keyser BM, Taylor JT (2005) Towards selective antagonists of T-type calcium channels: design, characterization and potential applications of NNC 55-0396. *Cardiovasc Drug Rev* 23:173–96
- Liao P, Yu D, Li G, Yong TF, Soon JL, Chua YL, Soong TW (2007) A smooth muscle Cav1.2 calcium channel splice variant underlies hyperpolarized window current and enhanced state-dependent inhibition by nifedipine. *J Biol Chem* 282:35133–42
- McHugh D, Beech DJ (1996) Modulation of Ca²⁺ channel activity by ATP metabolism and internal Mg²⁺ in guinea-pig basilar artery smooth muscle cells. *J Physiol* 492:359–76
- Moosmang S, Haider N, Bruderl B, Welling A, Hofmann F (2006) Antihypertensive effects of the putative T-type calcium channel antagonist mibefradil are mediated by the L-type calcium channel Cav1.2. *Circ Res* 98:105–10
- Moosmang S, Schulla V, Welling A, Feil R, Feil S, Wegener JW, Hofmann F, Klugbauer N (2003) Dominant role of smooth muscle L-type calcium channel Cav1.2 for blood pressure regulation. *EMBO J* 22:6027–34
- Morita H, Cousins H, Onoue H, Ito Y, Inoue R (1999) Predominant distribution of nifedipine-insensitive,

- high voltage-activated Ca^{2+} channels in the terminal mesenteric artery of guinea pig. *Circ Res* 85: 596–605
- Morita H, Shi J, Ito Y, Inoue R (2002) T-channel-like pharmacological properties of high voltage-activated, nifedipine-insensitive Ca^{2+} currents in the rat terminal mesenteric artery. *Br J Pharmacol* 137:467–76
- Navarro-Gonzalez MF, Grayson TH, Meaney KR, Cribbs LL, Hill CE (2009) Non-L-type voltage-dependent calcium channels control vascular tone of the rat basilar artery. *Clin Exp Pharmacol Physiol* 36: 55–66
- Nikitina E, Zhang ZD, Kawashima A, Jahromi BS, Bouryi VA, Takahashi M, Xie A, Macdonald RL (2007) Voltage-dependent calcium channels of dog basilar artery. *J Physiol* 580:523–41
- Perez-Reyes E (2003) Molecular physiology of low-voltage-activated t-type calcium channels. *Physiol Rev* 83: 117–61
- Rodman DM, Reese K, Harral J, Fouty B, Wu S, West J, Hoedt-Miller M, Tada Y, Li KX, Cool C, Fagan K, Cribbs L (2005) Low-voltage-activated (T-type) calcium channels control proliferation of human pulmonary artery myocytes. *Circ Res* 96:864–72
- Shcheglovitov A, Kostyuk P, Shuba Y (2007) Selectivity signatures of three isoforms of recombinant T-type Ca^{2+} channels. *Biochim Biophys Acta* 1768:1406–19
- Shcheglovitov A, Vitko I, Bidaud I, Baumgart JP, Navarro-Gonzalez MF, Grayson TH, Lory P, Hill CE, Perez-Reyes E (2008) Alternative splicing within the I-II loop controls surface expression of T-type $\text{Ca}(\text{v})3.1$ calcium channels. *FEBS Lett* 582:3765–70
- Tomassoni D, Lanari A, Silvestrelli G, Traini E, Amenta F (2008) Nimodipine and its use in cerebrovascular disease: evidence from recent preclinical and controlled clinical studies. *Clin Exp Hypertens* 30:744–66
- Vacher E, Richer C, Fornes P, Clozel JP, Giudicelli JF (1996) Mibefradil, a selective calcium T-channel blocker, in stroke-prone spontaneously hypertensive rats. *J Cardiovasc Pharmacol* 27:686–94
- Van der Vring JA, Cleophas TJ, Van der Wall EE, Niemeyer MG (1999) T-channel-selective calcium channel blockade: a promising therapeutic possibility, only preliminarily tested so far: a review of published data. T-Channel Calcium Channel Blocker Study Group. *Am J Ther* 6:229–33
- VanBavel E, Sorop O, Andreasen D, Pfaffendorf M, Jensen BL (2002) Role of T-type calcium channels in myogenic tone of skeletal muscle resistance arteries. *Am J Physiol Heart Circ Physiol* 283:H2239–43
- Welling A, Ludwig A, Zimmer S, Klugbauer N, Flockerzi V, Hofmann F (1997) Alternatively spliced IS6 segments of the alpha 1C gene determine the tissue-specific dihydropyridine sensitivity of cardiac and vascular smooth muscle L-type Ca^{2+} channels. *Circ Res* 81:526–32
- Wolfe SE, Navarro-Gonzalez MF, Grayson TH, Stricker C, Hill CE (2010) Involvement of nonselective cation channels in the depolarisation initiating vasomotion. *Clin Exp Pharmacol Physiol*; doi: 10.1111/J.1440-1681.2009.05350.x (in press)
- Worley JF, Quayle JM, Standen NB, Nelson MT (1991) Regulation of single calcium channels in cerebral arteries by voltage, serotonin, and dihydropyridines. *Am J Physiol* 261:H1951–60

Supplementary Information accompanies the paper on the Journal of Cerebral Blood Flow & Metabolism website (<http://www.nature.com/jcbfm>)